

5. Hu Hang, Deng Xinhong, An Improved LCMV Method at Subarray Level, Proceedings of the IET International Conference on Wireless, Mobile and Multimedia Networks, Hangzhou, 2006, pp. 1-4.
6. A. Pezeshki, B. D. Van Veen, L. L. Scharf. Eigenvalue beamforming using a multirank MVDR beamformer and subspace selection. IEEE Transactions on Signal Processing, 2008, 56, p.p.1954-1967.
7. Y. H. Choi. Robust adaptive array using Taylor series expansion. Electronics Letters, 2011, 47, p.p. 840-841.
8. Jiang Xue, Zeng Wenjun, A. Yasocharan, C. S. Hing, T. Kirubarajan. Quadratically constrained minimum dispersion beamforming via gradient projection. IEEE Transactions on Signal Processing, 2015, 63, p.p.192-205.
9. C. H. Hsu, M. C. Hua, H. H. Hsu, H. C. Liu, Robust pointing error compensation technique based on rooting method for CDMA signals, Proceedings of the International Symposium on Communication Systems, Networks & Digital Signal Processing, Poznan, 2012, pp.1-4.
10. Yan Fei, Zhao Shumin. Robust LCMV Beamformer Algorithm Based on Steepest Descent Method, Computer Simulation, 2012, 29, p.p.117-120.
11. Fan Zhan, Liang Guolong, Wang Yilin. Robust adaptive beamforming with null widening. Journal of Electronics & Information Technology, 2013, 35, p.p. 2764-2770.
12. Yang Tao, Su Tao, He Xuehui. Robust adaptive beamforming based on beamspace steering vector estimation. Journal of Electronics & Information Technology, 2013, 35, p.p.2758-2763.
13. Gu Yujie, N. A. Goodman, S. Hong, Li Yu. Robust adaptive beamforming based on interference covariance matrix sparse reconstruction. Signal Processing, 2014, 96, p.p.375-381.
14. Xie Julan, Li Huiyong, He Zishu, Li Chaohai. A robust adaptive beamforming method based on the matrix reconstruction against a large DOA mismatch. EURASIP Journal on Advances in Signal Processing, 2014, 91, p.p.1-10.
15. L. Du, J. Li, P. Stoica. Fully automatic computation of diagonal loading levels for robust adaptive beamforming. IEEE Transactions on Aerospace and Electronic Systems, 2010, 46, p.p.449-458.



The Research on the Model of Image Denoising Based on the Fusion of Anisotropic Diffusion and Total Variation Models

Yang Tang^{1*}, Fang Li^{2,3}

1 Department of Computer Science, Chongqing Electric Power College, Chongqing, 400053, China

2 College of Computer Science, Chongqing University, Chongqing, 400044, China

3 Chongqing City Management College, Chongqing, 401331, China

Abstract

In this paper, the author researched on the model of image denoising based on the fusion of anisotropic diffusion and total variation models. The noise is present at almost all data. The noise can degrade image quality, as a result the interpretations and analysis of the image will be much harder. Denoising is the process of reducing the noise.

The topic of denoising has attracted the attention of the majority of researchers in the field of image processing. The efforts of researchers have contributed to the innovation and development of several of denoising techniques. The multi-resolution geometry analysis, which is based on wavelet theory, has attracted a lot of attention. In spite of this, wavelet transform suffers from some drawbacks such as poor directional selectivity and absence of phase information.

Keywords: MODEL, FUSION OF ANISOTROPIC DIFFUSION, TOTAL VARIATION MODEL, IMAGE QUALITY

1. Introduction

An image is usually corrupted by noise in its acquisition and transmission. The degraded image severely affects the following image processing, such as image super resolution, image segmentation, image recognition, feature extraction. Thus, image denoising becomes a fundamental and important image processing for improving the quality of image. The goal of image denoising is to get a clearer and richer detailed image. Preserving the important structures such as edges and textures has important theoretical significance and application values. It is well-known that image structures are important for visual perception.

Hence, Chen's paper [1] mainly focuses on image denoising model for edge-preservation and texture-preservation. Several new image denoising methods are proposed based on wavelet transform, kernel regression and nonlocal means, respectively. Using the scale correlation and maxima modulus of wavelet coefficients, Jin [2] defines two new wavelet correlation coefficients based on maxima child nodes, and propose a new scale correlation based image denoising method. Sun [3] extends these definitions to fractional B-spline wavelet coefficients. Both theoretical and experimental results demonstrate that the proposed correlation coefficients can capture the structure information in high frequency sub bands. So more edges and textures are kept in the denoised image and the quality of denoised image is improved. To overcome the shortcomings of the regularity exponent based image denoising model, a new image denoising model combining the regularity exponent and image total variation (TV) is proposed. The model fully utilizes the relationship between wavelet coefficients and signal regularity. So the image regularity is modified by changing the wavelet coefficients in different scales. The noise is reduced while sharp edges are preserved; meanwhile, the Gibbs phenomenon is disappeared. With the fractional B-spline wavelet instead of the traditional wavelet, Wu [4] establishes a denoising algorithm based on the fractional B-spline wavelet and total variation. In this case, edges and textures are both maintained in the denoised image. An adap-

tive kernel regression model based on structure tensor is proposed. The structure tensor, which can exploit the local gradient structure information, provides information to achieve a data-adaptive kernel function. Due to the accurate estimation of edge orientations, edges and textures structure information are well preserved and a better visual effects are achieved during denoising and interpolation. Meanwhile, the RMSE is also proved the effectiveness of the algorithm. To overcome the shortcomings of Steering kernel regression, two more robust kernel functions are applied to kernel regression, which are robust to micro-edges. On the image edges, the kernel functions have a faster decay, and the weight of pixels are assigned a small value. Thus it discourages the pseudo-edges. Experimental results of image denoising and interpolation show that the efficiency of the proposed models, especially to the image with less textures and more edge details. Yu [5] proposes a novel nonlocal TV variation model, where the fidelity term is based on the Patch similarity, and regularity term is nonlocal TV priori. The iterative nonlocal provides structure similarity between noisy and denoised images; while the nonlocal TV preserves the edge and texture details. Compared with other related denoising methods, the proposed model can preserve more structure information in denoised image, especially to the image with much noise. Combining the nonlocal Patch similarity regularization with TV regularization, Yang [6] proposes a new nonlocal Patch self-similarity regularized image denoising model. The similarity of Patches are said to be accurate, by introducing adaptive structure tensor to compute weight function of nonlocal Patch similarity. So in the denoised image, more structural features can be retained. A simpler and more effective algorithm, Split Bregman algorithm, is used to solve the model iteratively. By extending the model to image restoration, our model improves the quality of restoration image and the efficiency of computational complexity.

2. The Total Variation Model

The major problem of image processing is how to remove noise without blurring edges of the image. Commonly noise pertains to the high frequencies in

an image, and the image details (edge and tenure); principally appear also in regions of high frequencies. The most effective algorithm is the one that has the ability to solve this contradiction. More precisely, least diffusion is in the regions that potentially contain more image features, and most diffusion is in the regions that potentially contain less image features. Wherefore in our current work the gradient in each region of the image is calculated as a measure of the amount of image details.

In our image smoothing scheme, the image gradient Du keeps changing as the iterative evolution changes. Consequently, the threshold, which is used to determine either the region that is an edge or a flat area, should not be steady, but keeps changing with the number of iterations.

Image denoising is a basic topic in the field of image processing and computer vision. The aim of image denoising is to remove noise while preserving image details as much as possible. The existing image denoising methods are classified into local methods and nonlocal methods, the nonlocal means (NLM) methods as a brand-new image denoising strategy was proposed in recent years. The proposed algorithms obtain better image denoising results than the original NLM method and several existing NLM methods. Moreover, we pay close attention to the problem of impulse noise removal and extend NLM method to remove impulse noise from images. The proposed algorithm is capable of effectively suppressing any type of impulse noise and mixed impulse noise, in contrast to many existing methods which are specialized for impulse noise removal.

For detection, a robust local image statistic, called the extreme compression rank-order absolute difference (ECROAD), is designed to detect impulse noise in an image. For filtering, a universal impulse noise filter is proposed by combining ECROAD results with NLM filtering framework. The proposed impulse weight is able to avoid the effect of noisy pixels in computing similarity weight and restoring candidates. The patch-based similarity measure can provide higher correlation between the corrupted pixel and neighborhood pixel. Higher correlation gives rise to better noise suppression and edge preservation. Experimental results demonstrate that the proposed filter is efficiently able to suppress any type of impulse noise and mixed impulse noise, and outperforms other universal impulse noise filters and some existing filters which are specialized for different impulse noise models.⁴ We present two filters, noise adaptive edge-preserving filter (NAEPF) and noise adaptive switching bilateral filter (NASBF),

for removal of salt-and-pepper noise. For detection, two extreme intensity values are used to identify possible noise pixels. For filtering, NAEPF is first developed for noise suppression and details preserving. It adopts three different filtering techniques for noise removal and detail-preserving, switching filtering, edge-preserving filtering, and noise adaptive median filtering. Switching filtering can retain noise-free pixels unchanged. Edge-preserving filtering can preserve more image details. Noise adaptive median filtering can suppress high-level salt and pepper noise. Then, NASBF is proposed by combining noise detection results with NAEPF estimation.

The new function is continuous and has infinite rank continuous derivative. It is suitable for various mathematical processing. At the same time, the new function satisfies the shrinkage condition and it has adaptive character. These advantages make it possible to construct an adaptive algorithm for signal denoising. Moreover, computationally efficient formulas for computing bias, variance and risk of the adaptive thresholding function are derived. Some numerical experiments show the new function can preserve more significant information of original images and gives better performance in PSNR and visual quality.⁴ A novel image denoising algorithm is obtained by combining tartlet transform with Stein's unbiased risk estimate approach. Hence, it integrates the advantages of two methods. This approach took advantage of a multi-scale framework and directionality of tartlet transform to preserve the significant information of original image like edges and details. And Stein's unbiased risk estimate approach denoises an image by minimizing the mean squared error (MSE) between the clean image and the denoised one. It is unnecessary to set a known thresholding. Numerical results show the effectiveness of our technique.

Two parameters for optimal threshold function are obtained from niche adaptive genetic algorithms. Based on crowding mechanism, punishing function is adopted to adjust individual fitness and advance global capability. We minimize an estimate of the mean square error by using genetic algorithm. Numerical experiments show that the proposed new algorithm is very effective in adaptively finding the optimal solution in mean square error sense.⁶ Image quality improving techniques based on partial differential equations are famous for the capability of denoising while keeping edges sharp because of the different filters in edges and inner area. Combined with the multi-scale transform, a new image denoising model is proposed with better results for human vision characteristics. The new model has got excellent experiment results

of denoising while keeping texture and geometry structure unfading.

3. The Fusion of Anisotropic Diffusion Algorithm

The basic equation is shown in the following equation (1) and (2):

$$\sigma_1 - \sigma_3 = \frac{(a + c\varepsilon_1)\varepsilon_1}{(a + b\varepsilon_1)^2} \quad (1)$$

$$\sigma_1 - \sigma_3 = \frac{(a\varepsilon_1 + c)\varepsilon_1}{(a + b\varepsilon_1)^2} \quad (2)$$

where, $\sigma_1 - \sigma_3$ refers to the optimization parameter; ε_1 is the axial strain; and a, b, c are fitting parameters. The boundary conditions are shown in Eq. 3:

$$\left\{ \begin{array}{l} \frac{d(\sigma_1 - \sigma_3)}{d\varepsilon} \Big|_{\varepsilon=0} = E_0 \\ (\sigma_1 - \sigma_3) \Big|_{\varepsilon=\varepsilon_{\max}} = (\sigma_1 - \sigma_3)_{\max} \\ \frac{d(\sigma_1 - \sigma_3)}{d\varepsilon} \Big|_{\varepsilon=\varepsilon_{\max}} = 0 \end{array} \right. \quad (3)$$

where E_0 is the initial elastic modulus of BFRS; ε_{\max} is the maximum strain; and $(\sigma_1 - \sigma_3)_{\max}$ refers to the maximum deviatoric stress.

Substituting Eq. 2 to Eq. 3, we can obtain

$$\begin{aligned} & [4(\sigma_1 - \sigma_3)_{\max} E_0^2 - E_0^3 \varepsilon_1] a^2 \\ & + [8(\sigma_1 - \sigma_3)_{\max} E_0 \varepsilon_{\max} - (E_0 \varepsilon_{\max})^2] a \\ & + 4(\sigma_1 - \sigma_3)_{\max} \varepsilon_{\max}^2 = 0 \end{aligned} \quad (4)$$

Eq. 4 indicates that the maximum deviatoric parameter which is determined by parameter a. Parameters m, n, p can be defined as follows:

$$\left\{ \begin{array}{l} 4(\sigma_1 - \sigma_3)_{\max} E_0^2 - E_0^3 \varepsilon_1 = \frac{m}{2} \\ (E_0 \varepsilon_{\max})^2 - 8(\sigma_1 - \sigma_3)_{\max} E_0 \varepsilon_{\max} = n \\ 4(\sigma_1 - \sigma_3)_{\max} \varepsilon_{\max}^2 = p \end{array} \right. \quad (5)$$

Therefore,

$$\left\{ \begin{array}{l} a = \frac{n \pm \sqrt{n^2 - 2mp}}{m} \\ b = \frac{2}{E_0} + \frac{n \pm \sqrt{n^2 - 2mp}}{m\varepsilon_1} \\ c = E_0 \left(\frac{n \pm \sqrt{n^2 - 2mp}}{m} \right)^2 \end{array} \right. \quad (6)$$

The model is adopted to describe the curves in these conditions, and the equation is shown as follows:

$$\sigma_1 - \sigma_3 = \frac{\varepsilon_1}{a + b\varepsilon_1} \quad (7)$$

where

$$a = \frac{1}{\left(\frac{\sigma_1 - \sigma_3}{\varepsilon_1} \right)_{\varepsilon_1 \rightarrow 0}} = \frac{1}{E_0} \quad (8)$$

$$b = \frac{1}{(\sigma_1 - \sigma_3)_{\varepsilon_1 \rightarrow \infty}} = \frac{1}{(\sigma_1 - \sigma_3)_{\max}} \quad (9)$$

The above two conditions can be expressed as follows:

$$\exists u \in N, c(P_{us}^*) < B/2 \quad (10)$$

$$\sum_{u \in N} r(u) / |N| < B/2 \quad (11)$$

Correspondingly, the weight coefficient ω_k is defined as follows:

$$\omega_k = \min \{ c(P_{us}^*) \mid u \in N_k \} \quad (12)$$

Therefore, the relocation direction is as follows:

$$Dr = \left\{ k \mid \max_{1 \leq k \leq 4} \{ \omega_k \} \right\} \quad (13)$$

Afterwards, the optimization problem is described as follows.

$$J(w, e) = \frac{w^T w}{2} + \frac{\lambda}{2} \cdot \sum_{i=1}^N e_i^2 \quad (14)$$

where the following equality constraints should be satisfied.

$$y(x) = w^T \cdot \zeta(x_i) + b + e_i, i \in \{1, 2, \dots, N\} \quad (15)$$

Afterwards, the Lagrangian function is defined as follows.

$$\begin{aligned} \delta(w, b, e, \alpha) &= \frac{w^T w}{2} + \frac{\lambda}{2} \cdot \sum_{i=1}^N e_i^2 \\ &- \sum_{i=1}^N \alpha_i (w^T \zeta(x_i) + b + e_i - y_i) \end{aligned} \quad (16)$$

In Eq.4, α_i represents denotes the Lagrange multipliers that can either be positive or negative state under the equality constraints, so we have:

$$\frac{\partial \delta}{\partial w} = 0 \rightarrow w = \sum_{i=1}^N \alpha_i \cdot \zeta(x_i) \quad (17)$$

$$\frac{\partial \delta}{\partial b} = 0 \rightarrow \sum_{i=1}^N \alpha_i = 0 \quad (18)$$

$$\frac{\partial \delta}{\partial e_i} = 0 \rightarrow \alpha_i = \lambda_i \cdot e_i, i \in \{1, 2, \dots, N\} \quad (19)$$

$$\frac{\partial \delta}{\partial \alpha_i} = 0 \rightarrow y_i = w^T \cdot \zeta(x_i) + b + e_i \quad (20)$$

Particularly, in each iteration, fitness functions are evaluated for all particles and then the number of iterations is obtained as follows.

$$x^i = (x^{i1}, x^{i2}, \dots, x^{iD}) \quad (21)$$

$$v^i = (v^{i1}, v^{i2}, \dots, v^{iD}) \quad (22)$$

Therefore, a specific can be updated by the following two equations.

$$v_{k+1}^i = w_k \cdot v_k^i + s_1 \cdot t_1 \cdot (p_{best} - x_k^i) + s_2 \cdot t_2 \cdot (g_{best} - x_k^i) \quad (23)$$

$$x_{k+1}^i = x_k^i + v_{k+1}^i \quad (24)$$

Parameter w_k refers to the inertia weight, it can be calculated as follows.

$$w_k = w_{max} - \frac{k-1}{K} \cdot (w_{max} - w_{min}) \quad (25)$$

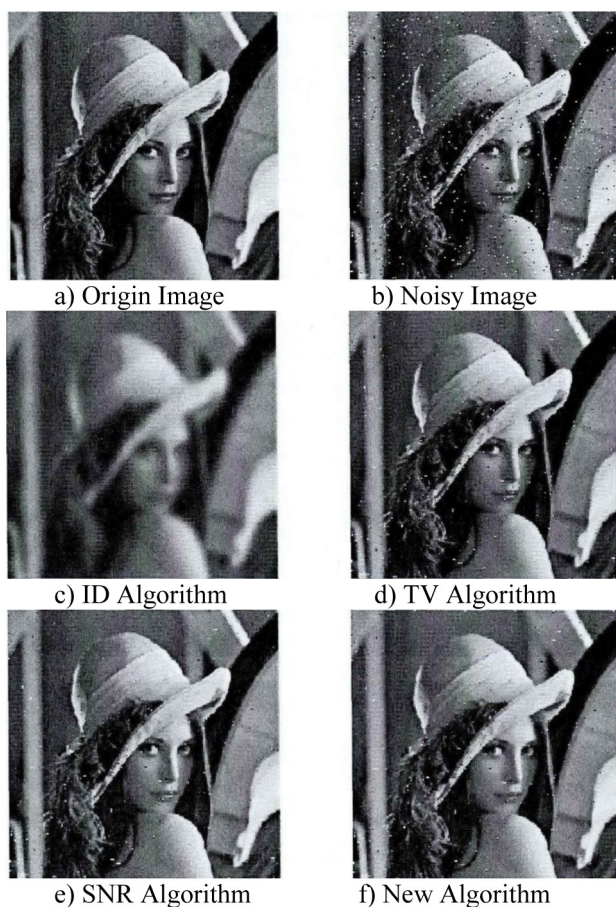


Figure 1. Results of denoising obtained with Lena image (256 x 256 bit)

4. The Experiment Analysis

To evaluate the proposed algorithm, we select Lena Cameraman and Boat images as examples. In our experiments, we pollute Lena image by salt and pepper noise, while Cameraman and Boat images are polluted by white Gaussian noise. The experimental results are shown in Figures 1-3, where in each figure is described respectively the original image, the noisy image, and the results by: the ID algorithm, the TV algorithm, the Ref algorithm, and our new algorithm. The results of the new algorithm are compared with those of ID algorithm, TV algorithm and new algorithm. In our experiments the parameters are selected as follows: the time step size $\Delta t=0.1$, the grid step size $h=1$, $\lambda=0.01$, $k_0=15$, and the number of iteration $N=50$.

Figures 1-3 show that the new model has the best impact on the denoising among the four models, since it not only maintains the advantages of the isotropic diffusion model, TV model, but also overcomes the disadvantage of the two models.

This verifies the superiority of our model in terms of removing noise and preserving edges of the image. From figures 1 and 2 we can discern that the quantitative assessments (PSNRs and SSIMs) of the four

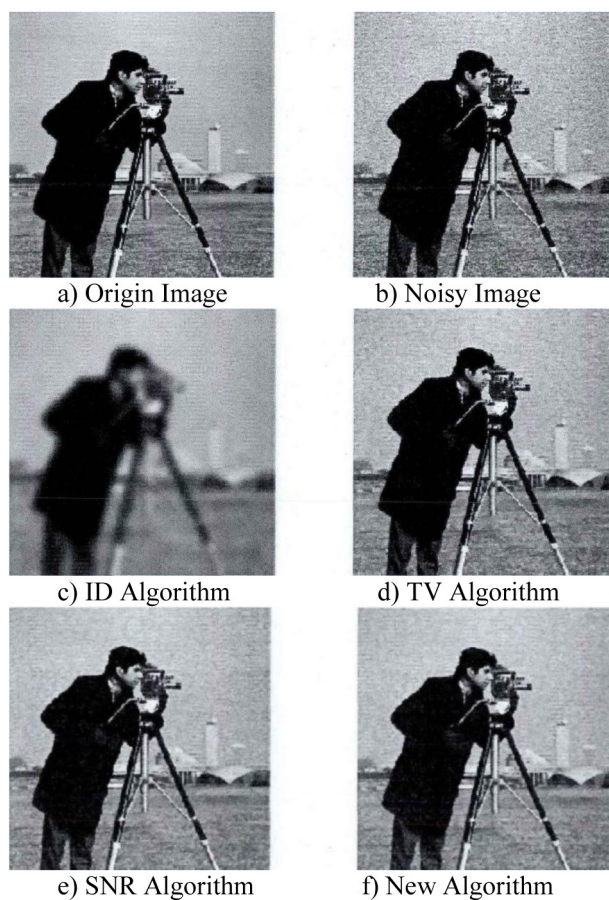


Figure 2. Results of denoising obtained with cameraman image (256 x 256 bit)

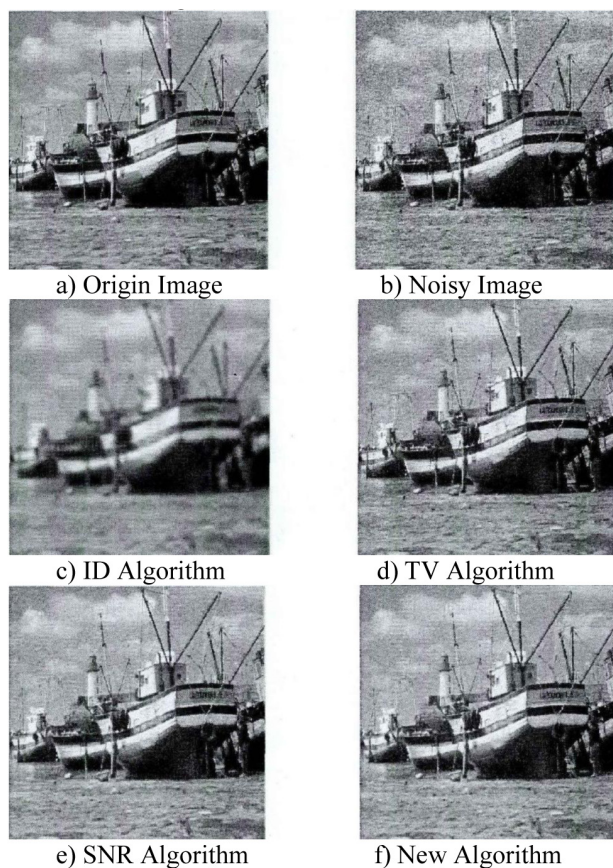


Figure 3. Results of denoising obtained with boat image (256 x 256 bit)

algorithms decrease as the variance of the noise increases. Nonetheless the values of PSNR and SSIM of the new model are the best (highest) among the four algorithms for the same variance.

Figures 2 and 3 show the relationship between the variance of the noise and both of PSNRs and SSIMs respectively, from which we can see that the PSNRs and SSIMs for the new model are the highest among the four models.

The algorithm proposed in this paper can be implemented as follows:

- Step 1. Input observed image u_0
- Step 2. Set values of the initial parameters $h, \lambda, \Delta t, k_0$ and the iteration number $N, n=1, u=u_0$
- Step 3. Calculate K by (3.3.3).
- Step 4. Calculate the image gradient magnitude.
- Step 5. Calculate θ by (3.3.2).
- Step 6. Calculate η by (3.3.4).
- Step 7. Calculate
- Step 8. $n=n+1$
- Step 9. Output. if $n < N$, return to step 4.

Conclusions

In this paper, the author researched on the model of image denoising based on the fusion of anisotropic diffusion and total variation models. Commonly noise pertains to the high frequencies in an image,

and the image details (edge and tenure); principally appear also in regions of high frequencies. The most effective algorithm is the one that has the ability to solve this contradiction. More precisely, least diffusion is in the regions that potentially contain more image features, and most diffusion is in the regions that potentially contain less image features. Wherefore in our current work the gradient in each region of the image is calculated as a measure of the amount of image details. To evaluate the proposed algorithm, we select Lena Cameraman and Boat images as examples. In our experiments, we pollute Lena image by salt and pepper noise, while Cameraman and Boat images are polluted by white Gaussian noise. The result shows that the model of the fusion of anisotropic diffusion and total variation models can achieve better performance in image denoising.

Acknowledgements

This work is supported by the Key Project of State Grid Chongqing Electric Power Company, China (No.201566), and the Chongqing Municipal Education Commission scientific and technological research project, China (No.KJ1503209).

References

1. Shifeng Chen, Ming Liu, Wei Zhang, Jianzhuang Liu. Edge preserving image denoising with a closed form solution. *Pattern Recognition*, 2013, pp. 463-471.
2. Jianqiu Jin, Bailing Yang, Kewei Liang, Xun Wang. General image denoising framework based on compressive sensing theory. *Computers & Graphics*, 2014, pp. 38-48.
3. Dong Sun, Qingwei Gao, Yixiang Lu, Zhixiang Huang, Teng Li. A novel image denoising algorithm using linear Bayesian MAP estimation based on sparse representation. *Signal Processing*, 2014, pp. 667-684.
4. Yue Wu, Brian H. Tracey, Premkumar Natarajan, Joseph P. Noonan. Fast block wise SURE shrinkage for image denoising. *Signal Processing*, 2014, pp. 129-137.
5. Zhiyong Zuo, Tianxu Zhang, Xia Lan, Li Liu, Jing Hu. Content-based adaptive image denoising using spatial information. *Optik - International Journal for Light and Electron Optics*, 2014, pp. 543-549.
6. Chong Yu, Xiong Chen. Remote sensing image denoising application by generalized morphological component analysis. *International Journal of Applied Earth Observations and Geo-information*, 2014, pp. 419-428.

7. Xiang-Yang Wang, Yang-Cheng Liu, Hong-Ying Yang. Image denoising in extended Shearlet domain using hidden Markov tree models. *Digital Signal Processing*, 2014, pp. 30-41.
8. Hong-Ying Yang, Xiang-Yang Wang, Pan-Pan Niu, Yang-Cheng Liu. Image denoising using non subsampled shearlet transform and twin support vector machines. *Neural Networks*, 2014, pp. 57-69.



Research on High Frequency Dynamic Bridge Deflection Detection Based on Digital Imaging

Yude Xiao^{*1}, Shaowen Sun², Qiang Guo³, Guoxi Tang⁴

1.Anhui Communications Vocational & Technical College, 230051, Hefei, China*

2. Anhui Water Resources Department, 230022, Hefei, China

3. Anhui Communications Vocational & Technical College, 230051, Hefei, China

4. Anhui Transport Consulting & Design Institute Co., Ltd, 230088, Hefei, China

Abstract

This paper presents a measurement method of dynamic bridge deflection detection in high frequency based on digital imaging technology. This system based on digital imaging theory and the hardware including matrix camera, long telephoto lens, laser rangefinder, target markers, auxiliary lighting, and industrial tablet. Target markers were continuously collected by the camera in high frequency, wirelessly transferred to industrial tablet. Based on the algorithm of HALCON, target images were recognized by user application program which is developed under Visual Studio 2010 C++. By calculating the center position of the target image, the target markers displacement is achieved. Experiments show that the method can achieve the detection accuracy of 0.1 mm and this method is characterized with non-contact, remote and dynamic automated detection, high precision, etc.

Keywords: DEFLECTION, BRIDGE, IMAGING, CAMERA, DYNAMIC

1. Introduction

Deflection is a very important indicator in bridge security evaluation, which directly reflects the carrying capacity of the bridge structure. The value of bridge deflection needs to be measured accurately in both static and dynamic state in bridge test, as well as unsafe bridge renovation and new bridge acceptance. The impact coefficient and structural internal

force distribution of loads can be drawn from numerical analysis of dynamic deflection to determine the integrity of the weak parts of bridges [1]. Traditional bridge deflection detecting methods are as follows: dial indicator, level gauge and theodolite. Modern measurement ways include line CCD, total station instrument, communication pipe, inclinometers, laser imaging, and differential GPS [2-4].